Approximated Solutions on the Electromagnetic Field in Near Zone Generated by a Horizontal Electric Dipole on the Planar Surface of the Anisotropic Rock

Tingting Gu, Honglei Xu, and Kai Li

College of Information Science and Electronic Engineering
Zhejiang University, Hangzhou, 310027, China
ttgu@zju.edu.cn, hongleixu@zju.edu.cn, kaili@zju.edu.cn

Abstract ─ In this paper, the approximate formulas have been derived for ELF electromagnetic field in near zone from a horizontal electric dipole on the surface of sea water and one-dimensional anisotropic rock boundary. The computational scheme exploits the concept of quasi-static approach for ELF near-field approximations. Specifically, the integrands of Fourier-Bessel representations are approximated by adopting Maclaurin's Expansion where the ratio of wave numbers for rock and sea approaches zero. The approximated solution is in good agreement with the available experimental data.

Index Terms ─ Anisotropic rock horizontal, ELF near-field, electric dipole.

I. INTRODUCTION

The electromagnetic fields generated by a vertical electric dipole or a horizontal electric dipole near the boundary between two different media like earth and air or sea water and rock have been known in terms of analytical closed-form expressions for decades [1].

In order to evaluate these formulas, extensive studies have been made by many investigators through analytical [2-15] and numerical techniques [16-21]. Among many applied frequency bands, the ELF wave (ELF: ranges from 3 Hz to 30 Hz) has been widely used to the fields, such as deep underground exploration, submarine prospection and communication evaluation. Unfortunately, most available formulas are not used in the ELF frequencies, where the integrands have divergent terms in near zone for ELF field. Additionally, difficulties to implement in the near-field region for ELF waves arise in numerical solution because of limited resolutions near the source.

Recently, this old problem was revisited by Pan [22] in Chapter 6 of the book where the ELF near-field wave propagation is investigated in its application to marine controlled-source electromagnetics (mCSEM) method. The computational scheme is developed from the approximated formulas in the book [5] by retaining fundamental terms. As an extension of these works, the approximate formulas for ELF wave have been derived to evaluate the Sommerfeld's integrals for in near zone in the presence of half-spaces. Since it is found in some stratified rock that the conductivity is anisotropic which consists of alternating layers of dense rock and less dense rock. Specially, the conductivity transverse to the bedding surfaces is always smaller than the conductivity parallel to the surfaces [23]. This motivates us to develop the stratified prototype, where the rock layer is seen as one-dimensionally anisotropic medium.

In the present study, the approximate expressions of ELF field components due to a horizontal electric dipole is addressed near the planar surface of the anisotropic rock with analytical approximations. Specifically, the quasi-static approach is adopted for ELF waves by $\gamma_2 \approx i\lambda$ in evaluations because the permittivity of sea water can be approximated by the pure imaginary function of frequency ($\varepsilon_{sea} \approx -i\sigma_{sea}/\omega$) when the operating frequencies are in the range of ELF frequencies. The nature of the approximation is on basis of the asymptotic expansions of integrands of the Fourier-Bessel representations near the poles. In what follows, the near-field electromagnetic field by the conditions of $k\rho << 1$, $z/\rho << 1$, $d/\rho << 1$, the ratio of wave numbers for rock and sea $|k_2/k_1|$ (subscripts 1 and 2 represent for sea water and rock, respectively) is equivalent to an infinitesimal $|k_2^2\gamma_1|/|k_1^2\gamma_2|$. The computational evaluations of ELF field in near zone are carried out along the planar surface of anisotropic rock with the approximated formulas. The time dependence $e^{-i\omega t}$ is suppressed throughout the analysis.

II. FORMULATIONS

A. Fourier-Bessel representations for ELF near field in the sea water along the surface of one-dimensional anisotropic rock

The relevant geometry is shown in Fig. 1, where the horizontal electric dipole in the $\hat{z}$ direction is

Submitted On: March 20, 2018
Accepted On: December 25, 2018

located at (0, 0, d). The above half space is Region 1 ($z \geqslant 0$) filled with sea water, and Region 2 is the ocean floor by the permittivity μ_0, permittivity $\varepsilon_{2x}=\varepsilon_{2y}$ and ε_{2z}, and conductivity $\sigma_{2x}=\sigma_{2y}$ and σ_{2z}. Then, the complex permittivities $\tilde{\varepsilon}_1$ and $\bar{\bar{\varepsilon}}_2$ are expressed as follows:

$$\tilde{\varepsilon}_1=\varepsilon_0(\varepsilon_{r1}-i\frac{\sigma_{sea}}{\omega\varepsilon_0}), \qquad (1)$$

$$\bar{\bar{\varepsilon}}_2=\varepsilon_0\bar{\bar{\varepsilon}}_{r2}=\varepsilon_0\begin{bmatrix}\varepsilon_{rT}-i\frac{\sigma_T}{\omega\varepsilon_0} & 0 & 0\\ 0 & \varepsilon_{rT}-i\frac{\sigma_T}{\omega\varepsilon_0} & 0\\ 0 & 0 & \varepsilon_{rL}-i\frac{\sigma_L}{\omega\varepsilon_0}\end{bmatrix}. \qquad (2)$$

With the time dependence $e^{-i\omega t}$, the Maxwell's equations in the two half-spaces are represented by:

$$\nabla\times\boldsymbol{E}_j=i\omega\boldsymbol{B}_j, \qquad (3)$$

$$\nabla\times\boldsymbol{B}_j=\mu_0(-i\omega\hat{\varepsilon}_j\boldsymbol{E}_j+\hat{x}J_x^e), \qquad (4)$$

where j = 1, 2, and,

$$J_x^e=Idl\delta(x)\delta(y)\delta(z-d), \qquad (5)$$

representing for the volume current density in the dipole.

The Fourier transform is in the form of,

$$\boldsymbol{E}(x,y,z)=\frac{1}{(2\pi)^2}\int_{-\infty}^{+\infty}\mathrm{d}\xi\int_{-\infty}^{+\infty}\mathrm{d}\eta\mathrm{e}^{i(\xi x+\eta y)}\tilde{E}(\xi,\eta,z), \qquad (6)$$

and similar transform for $\boldsymbol{B}(x, y, z)$ and J_x^e are applied to Maxwell's equation. Then, we have:

$$\tilde{J}_x^e=I\mathrm{d}l\delta(z-d). \qquad (7)$$

In [22], the six Fourier integrals for ELF wave components of the electromagnetic field in Region 1 in the range $0 \le z \le d$ can be expressed as follows:

$$E_{1x}=\frac{Idl}{(2\pi)^2}\int_{-\infty}^{\infty}d\xi\int_{-\infty}^{\infty}d\eta e^{i(\xi x+\eta y)}\times\left(\left\{\lambda^2N_e+\xi^2\left[\gamma_1(\gamma_T\gamma_e-k_T^2)-\lambda^2\gamma_e\right]\right\}-\frac{e^{i\gamma_1 d}}{i\omega\tilde{\varepsilon}_1\gamma_1}\sin\gamma_1 z\right), \qquad (8)$$

$$E_{1y}=\frac{Idl}{(2\pi)^2}\int_{-\infty}^{\infty}d\xi\int_{-\infty}^{\infty}d\eta\xi\eta e^{i(\xi x+\eta y)}\times\left[\frac{\omega\mu_0 e^{i\gamma_1(z+d)}}{\lambda^2M_TN_e}(k_T^2\gamma_1+\lambda^2\gamma_e-\gamma_1\gamma_T\gamma_e)+\frac{e^{i\gamma_1 d}}{i\omega\tilde{\varepsilon}_1\gamma_1}\sin\gamma_1 z\right], \qquad (9)$$

$$E_{1z}=\frac{Idl}{(2\pi)^2}\int_{-\infty}^{\infty}d\xi\int_{-\infty}^{\infty}d\eta e^{i(\xi x+\eta y)}\xi\times\left[\frac{\omega\mu_0\gamma_e e^{i\gamma_1(z+d)}}{N_e}-\frac{e^{i\gamma_1 d}}{\omega\tilde{\varepsilon}_1}\cos\gamma_1 z\right], \qquad (10)$$

$$B_{1x}=-\frac{\mu_0 Idl}{(2\pi)^2}\int_{-\infty}^{\infty}d\xi\int_{-\infty}^{\infty}d\eta e^{i(\xi x+\eta y)}\xi\eta\times\frac{e^{i\gamma_1(z+d)}}{\lambda^2M_TN_e}(k_1^2\gamma_T\gamma_e-k_T^2\gamma_1^2), \qquad (11)$$

$$B_{1y}=-\frac{\mu_0 Idl}{(2\pi)^2}\int_{-\infty}^{\infty}d\xi\int_{-\infty}^{\infty}d\eta e^{i(\xi x+\eta y)}\times\left\{\frac{e^{i\gamma_1(z+d)}}{\lambda^2M_TN_e}\left[\lambda^2\gamma_1N_e+\xi^2(k_1^2\gamma_T\gamma_e-k_T^2\gamma_1^2)\right]-e^{i\gamma_1(z+d)}\cos\gamma_1 z\right\}, \qquad (12)$$

$$B_{1z}=\frac{\mu_0 Idl}{(2\pi)^2}\int_{-\infty}^{\infty}d\xi\int_{-\infty}^{\infty}d\eta e^{i(\xi x+\eta y)}\eta\times\left[\frac{e^{i\gamma_1(z+d)}}{M_T}-\frac{ie^{i\gamma_1 d}}{\gamma_1}\sin\gamma_1 z\right], \qquad (13)$$

where,

$$M_T=\gamma_1+\gamma_T, \qquad (14)$$

$$N_e=k_T^2\gamma_1+k_1^2\gamma_e=\frac{k_T}{k_L}(k_Lk_T\gamma_1+k_1^2\gamma_L), \qquad (15)$$

$$\gamma_T=\sqrt{k_T^2-\lambda^2}, \qquad (16)$$

$$\gamma_e=\sqrt{k_T^2-\frac{k_T^2}{k_L^2}\lambda^2}=\frac{k_T}{k_L}\gamma_L=\frac{k_T}{k_L}\sqrt{k_L^2-\lambda^2}, \qquad (17)$$

in which the square root is to be taken so that γ_n is in the first quadrant, and the upper sign "+" and the lower sign "-" correspond to $z>d$ and $0 \le z \le d$ in Region 1, respectively.

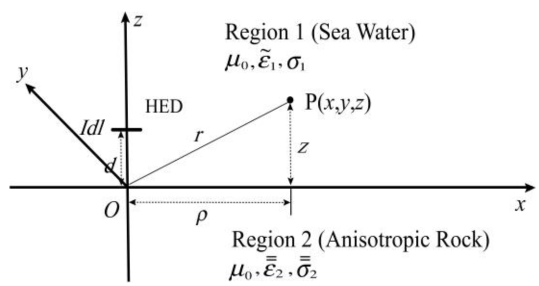

Fig. 1. The geometry for a unit horizontal electric dipole on the boundary between sea water and one-dimensional anisotropic rock.

The wave numbers of the regions are:

$$k_1=\omega\sqrt{\mu_0\varepsilon_0(\varepsilon_{r1}-i\sigma_{sea}/\omega\varepsilon_0)},$$
$$k_T=\omega\sqrt{\mu_0\varepsilon_0(\varepsilon_{rT}-i\sigma_T/\omega\varepsilon_0)},$$
$$k_L=\omega\sqrt{\mu_0\varepsilon_0(\varepsilon_{rL}-i\sigma_L/\omega\varepsilon_0)}, \qquad (18)$$

respectively. With the relations,

$$x=\rho\cos\varphi, \qquad y=\rho\sin\varphi,$$
$$\xi=\lambda\cos\varphi', \qquad \eta=\lambda\sin\varphi'. \qquad (19)$$

and the integral representation of the Bessel function of the first kind, viz.,

$$J_n(\lambda\rho)=\frac{i^{-n}}{2\pi}\int_0^{2\pi}e^{i\lambda\rho\cos\theta}e^{in\theta}d\theta. \qquad (20)$$

Thus, the final formulas of the six components in cylindrical coordinates (ρ, φ, z) in Region 1 can be expressed as follows:

$$E_{1\rho} = -\frac{\omega\mu_0 Idl}{4\pi k_1^2}\cos\varphi \times\left\{\int_0^\infty \left\{k_1^2 J_0(\lambda\rho) - \frac{1}{2}\lambda^2\left[J_0(\lambda\rho)-J_2(\lambda\rho)\right]\right\} \times\gamma_1^{-1}e^{i\gamma_1|z-d|}\lambda d\lambda + \int_0^\infty\left\{\frac{\gamma_1(k_1^2\gamma_e - k_T^2\gamma_1)}{2(k_1^2\gamma_e + k_T^2\gamma_1)}\left[J_0(\lambda\rho)-J_2(\lambda\rho)\right] - \frac{k_1^2(\gamma_T-\gamma_1)}{2\gamma_1(\gamma_T+\gamma_1)}\left[J_0(\lambda\rho)+J_2(\lambda\rho)\right]\right\}e^{i\gamma_1(z+d)}\lambda d\lambda\right\}, \quad (21)$$

$$E_{1\varphi} = \frac{\omega\mu_0 Idl}{4\pi k_1^2}\sin\varphi \times\left\{\int_0^\infty \left\{k_1^2 J_0(\lambda\rho) - \frac{1}{2}\lambda^2\left[J_0(\lambda\rho)+J_2(\lambda\rho)\right]\right\} \times\gamma_1^{-1}e^{i\gamma_1|z-d|}\lambda d\lambda + \int_0^\infty\left\{\frac{\gamma_1(k_1^2\gamma_e - k_T^2\gamma_1)}{2(k_1^2\gamma_e + k_T^2\gamma_1)}\left[J_0(\lambda\rho)+J_2(\lambda\rho)\right] - \frac{k_1^2(\gamma_T-\gamma_1)}{2\gamma_1(\gamma_T+\gamma_1)}\left[J_0(\lambda\rho)-J_2(\lambda\rho)\right]\right\}e^{i\gamma_1(z+d)}\lambda d\lambda\right\}, \quad (22)$$

$$E_{1z} = \frac{i\omega\mu_0 Idl}{4\pi k_1^2}\cos\varphi\times\left[\int_0^\infty(\pm e^{i\gamma_1|z-d|} + \frac{k_1^2\gamma_e - k_T^2\gamma_1}{k_1^2\gamma_e + k_T^2\gamma_1}e^{i\gamma_1(z+d)})\right] \times J_1(\lambda\rho)\lambda^2 d\lambda, \quad (23)$$

$$B_{1\rho} = -\frac{\mu_0 Idl}{4\pi}\sin\varphi\left\{\pm\int_0^\infty J_0(\lambda\rho)e^{i\gamma_1|z-d|}\lambda d\lambda + \int_0^\infty\left\{\frac{(k_1^2\gamma_e - k_T^2\gamma_1)}{2(k_1^2\gamma_e + k_T^2\gamma_1)}\left[J_0(\lambda\rho)+J_2(\lambda\rho)\right] - \frac{\gamma_T-\gamma_1}{2(\gamma_T+\gamma_1)}\left[J_0(\lambda\rho)-J_2(\lambda\rho)\right]\right\}e^{i\gamma_1(z+d)}\lambda d\lambda\right\}, \quad (24)$$

$$B_{1\varphi} = -\frac{\mu_0 Idl}{4\pi}\cos\varphi \times\left\{\pm\int_0^\infty J_0(\lambda\rho)e^{i\gamma_1|z-d|}\lambda d\lambda + \int_0^\infty\left\{\frac{(k_1^2\gamma_e - k_T^2\gamma_1)}{2(k_1^2\gamma_e + k_T^2\gamma_1)}\left[J_0(\lambda\rho)-J_2(\lambda\rho)\right] - \frac{\gamma_T-\gamma_1}{2(\gamma_T+\gamma_1)}\left[J_0(\lambda\rho)+J_2(\lambda\rho)\right]\right\}e^{i\gamma_1(z+d)}\lambda d\lambda\right\}, \quad (25)$$

$$B_{1z} = \frac{i\mu_0 Idl}{4\pi}\sin\varphi \times\left[\int_0^\infty(\pm e^{i\gamma_1|z-d|} - \frac{\gamma_T-\gamma_1}{\gamma_T+\gamma_1}e^{i\gamma_1(z+d)})\right]. \times\gamma_1^{-1}J_1(\lambda\rho)\lambda^2 d\lambda \quad (26)$$

B. Quasi-Static field approximation

In the range of ELF frequencies, the wavelength over a hundred thousand meters and the electric propagation distance subjected to $k_j\rho$<<1 make the problem a matter of ELF near-field propagation, where the integrands from equation (21) to equation (26) have divergent terms in the conventional sense. Since the operating frequency is enough low, the "quasi-static" approach is applied in similar manner addressed in [24] in order to evaluate these integrals in the near zone, with the following approximations:

(i) Considering that d<<ρ and z<<ρ where the dipole source height d and receiving height z are much less than the radial distance ρ, and $k_j\rho$<<1, where $j = T, L$, it is assumed that:

$$\gamma_j = \sqrt{k_j^2 - \lambda^2} = \lim_{\omega\to 0}\sqrt{(\frac{\varepsilon_{rj}^{1/2}}{c}\omega)^2 - \lambda^2} \approx i\lambda \cdot \quad (27)$$

(ii) The ratio of wave numbers for rock and sea k_j/k_1 is equivalent to an infinitesimal $|k_j^2\gamma_1|/|k_1^2\gamma_j|$.

(iii) High-order terms of the infinitesimals $k_j^2\gamma_1/k_1^2\gamma_j$ are allowed to be neglected for simplification as:

$$\frac{k_1^2\gamma_e - k_T^2\gamma_e}{k_1^2\gamma_e + k_T^2\gamma_e} = \frac{k_1^2\gamma_L - k_L k_T\gamma_1}{k_1^2\gamma_L + k_L k_T\gamma_1} \approx k_1^2 k_L k_T, \quad (28)$$

with,

$$\left|\frac{k_j^2\gamma_1}{k_1^2\gamma_j}\right| \approx \frac{\left|k_j^2\right|}{\left|k_1^2\right|}\frac{\left|\sqrt{k_1^2-\lambda^2}\right|}{|i\lambda|} \approx \left|\frac{k_j}{k_1}\right|\left|\sqrt{\left|\frac{k_j}{\lambda}\right|^2 - 1}\right| << 1. \quad (29)$$

It is seen that the integrands of F_1 to F_5 are divergent near the dipole source for what cannot be integrated directly. Consider that,

$$A(\lambda) = \frac{\gamma_T-\gamma_1}{\gamma_T+\gamma_1} = \frac{(\gamma_T-\gamma_1)^2}{(\gamma_T-\gamma_1)(\gamma_T+\gamma_1)} = \frac{(\gamma_T-\gamma_1)^2}{k_T^2 - k_1^2}. \quad (30)$$

In the near-field region,

$$\left|\gamma_T - \gamma_1 - k_1\right|d_m \approx \left|\sqrt{k_1^2-\lambda^2} - i\lambda - k_1\right|d_m \approx \xi\left|k_1 d_m\right| << 1, \quad (31)$$

where $\xi \subseteq [-1,1]$. Equation (31) can be approximated with by,

$$i(\gamma_T - \gamma_1 - k_1)d_m \approx 1 - e^{i(\gamma_T-\gamma_1-k_1)d_m}. \quad (32)$$

In addition, the function of $e^{i(\gamma_T-\gamma_1-k_1)d_m}$ is approximated by Maclaurin's expansion with first two orders retained, where:

$$e^{i(\gamma_T-\gamma_1-k_1)d_m} \approx 1 + i(\gamma_T-\gamma_1-k_1)d_m - \frac{((\gamma_T-\gamma_1-k_1)d_m)^2}{2!}, \quad -\infty < x < \infty. \quad (33)$$

Transpose the merger of similar items, we have:

$$(\gamma_T-\gamma_1)^2 = \frac{2}{d_m^2} - \frac{2e^{i(\gamma_T-\gamma_1-k_1)d_m}}{d_m^2} + \frac{2i(\gamma_T-\gamma_1-k_1)d_m}{d_m^2} - k_1^2 + 2k_1(\gamma_T-\gamma_1). \quad (34)$$

By invoking (32) and (33), it is derived that:

$$(\gamma_T-\gamma_1)^2 \approx 2ik_1\frac{1-e^{i(\gamma_T-\gamma_1-k_1)d_m}}{d_m} + k_1^2. \quad (35)$$

C. Approximated formulas for ELF field in near zone on the planar surface of anisotropic rock

The six components for electromagnetic field in equation (21) to equation (26) are approximated by:

$$E_{1\rho} \approx -\frac{\omega\mu_0 Idl}{4\pi k_1^2}\cos\varphi\Big[k_1^2 I_1(k_1,d_0) - \frac{1}{2}I_2(k_1,d_0) + \frac{k_1^2 k_L k_T}{2}I_9(k_1,d_1) - \frac{k_1^2}{2}F_1(d_1)\Big], \quad (36)$$

$$E_{1\varphi} \approx \frac{\omega\mu_0 Idl}{4\pi k_1^2}\sin\varphi\Big[k_1^2 I_1(k_1,d_0) - \frac{1}{2}I_2(k_1,d_0) + \frac{k_1^2 k_L k_T}{2}I_{10}(k_1,d_1) - \frac{k_1^2}{2}F_2(d_1)\Big], \quad (37)$$

$$E_{1z} \approx \frac{i\omega\mu_0 Idl}{4\pi k_1^2}\cos\varphi\Big[\pm I_4(k_1,d_0) + k_1^2 k_L k_T I_4(k_1,d_1)\Big] \quad \begin{cases}0\le z\le d\\ z>d\end{cases}, \quad (38)$$

$$B_{1\rho} \approx -\frac{\mu_0 Idl}{4\pi}\sin\varphi\Big[\pm I_5(k_1,d_0) + \frac{k_1^2 k_L k_T}{2}I_6(k_1,d_1) - \frac{1}{2}I_{13}(d_1)\Big] \quad \begin{cases}0\le z\le d\\ z>d\end{cases}, \quad (39)$$

$$B_{1\varphi} \approx -\frac{\mu_0 Idl}{4\pi}\cos\varphi\Big[\pm I_5(k_1,d_0) + \frac{k_1^2 k_L k_T}{2}I_7(k_1,d_1) - \frac{1}{2}F_4(d_1)\Big] \quad \begin{cases}0\le z\le d\\ z>d\end{cases}, \quad (40)$$

$$B_{1z} \approx \frac{i\mu_0 Idl}{4\pi}\sin\varphi\big[I_8(k_1,d_0) - F_5(d_1)\big], \quad (41)$$

in which the distances d_0, d_1 and r_0, r_1 are defined by:

$$d_0 = |z-d|, \qquad d_1 = z+d,$$
$$r_0 = \sqrt{d_0^2+\rho^2}, \quad r_1 = \sqrt{d_1^2+\rho^2}, \quad (42)$$

respectively. It is noted that the integrals I_1 to I_{10} have already been evaluated in [24]. The rest integrals F_1 to F_5 are to be evaluated, which are defined by:

$$F_1(d_1) = \int_0^\infty \{A(\lambda)[J_0(\lambda\rho)+J_2(\lambda\rho)]\}\gamma_1^{-1}e^{i\gamma_1 d_1}\lambda d\lambda, \quad (43)$$

$$F_2(d_1) = \int_0^\infty \{A(\lambda)[J_0(\lambda\rho)-J_2(\lambda\rho)]\}\gamma_1^{-1}e^{i\gamma_1 d_1}\lambda d\lambda, \quad (44)$$

$$F_3(d_1) = \int_0^\infty \{B(\lambda)[J_0(\lambda\rho)-J_2(\lambda\rho)]\}e^{i\gamma_1 d_1}\lambda d\lambda, \quad (45)$$

$$F_4(d_1) = \int_0^\infty \{B(\lambda)[J_0(\lambda\rho)+J_2(\lambda\rho)]\}e^{i\gamma_1 d_1}\lambda d\lambda, \quad (46)$$

$$F_5(d_1) = \int_0^\infty A(\lambda)J_1(\lambda\rho)e^{i\gamma_1 d_1}\gamma_1^{-1}\lambda^2 d\lambda, \quad (47)$$

where,

$$A(\lambda) = \frac{\gamma_T-\gamma_1}{\gamma_T+\gamma_1}, \quad B(\lambda) = \frac{\gamma_T-\gamma_1}{\gamma_T+\gamma_1}e^{i\gamma_1 z}. \quad (48)$$

Equation (48) is correspondingly expressed by

$$A(\lambda) = \frac{\gamma_T-\gamma_1}{\gamma_T+\gamma_1} = \frac{(\gamma_T-\gamma_1)^2}{k_T^2-k_1^2} \approx 2ik_1\frac{1-e^{i(\gamma_T-\gamma_1-k_1)d_m}}{(k_T^2-k_1^2)d_m} + \frac{k_1^2}{k_T^2-k_1^2}, \quad (49)$$

$$B(\lambda) \approx \left(2ik_1\frac{1-e^{i(\gamma_T-\gamma_1-k_1)d_m}}{(k_T^2-k_1^2)d_m} + \frac{k_1^2}{k_T^2-k_1^2}\right)e^{i\gamma_1 z}. \quad (50)$$

With the approximation by equation (49) and equation (50), F_1 to F_5 are simplified by superposition of several terms of I_1 to I_{10} so that the simplified representations for ELF electromagnetic wave near the horizontal electric dipole are readily obtained, where

$$F_1(d_m) \approx \frac{4i+2k_1 d_m}{(k_T^2-k_1^2)d_m\rho^2}\left(e^{ik_1 d_m}-e^{ik_1 r_m}\right) - \frac{4i}{(k_T^2-k_1^2)d_m\rho^2}\left(e^{ik_T d_m}-e^{ik_T r_m}\right), \quad (51)$$

$$F_2(d_m) \approx -\frac{4i+2k_1 d_m}{(k_T^2-k_1^2)d_m}\left[\frac{e^{ik_1 d_m}}{\rho^2} + \left(\frac{ik_1}{r_m}-\frac{1}{\rho^2}\right)e^{ik_1 r_m}\right] - \frac{4ik_1}{(k_T^2-k_1^2)k_T d_m}\left[\frac{e^{ik_T d_m}}{\rho^2} + \left(\frac{ik_T}{r_m}-\frac{1}{\rho^2}\right)e^{ik_T r_m}\right], \quad (52)$$

$$F_3(d_m) \approx -\frac{4ik_1+2k_1^2 d_m}{(k_T^2-k_1^2)d_m}\left[\frac{e^{ik_1 d_m}}{\rho^2} + \frac{d_m}{r_m}\left(\frac{ik_1}{r_m}-\frac{1}{r^2}-\frac{1}{\rho^2}\right)e^{ik_1 r_m}\right] + \frac{4ik_1}{(k_T^2-k_1^2)d_m}\left[\frac{e^{ik_T d_m}}{\rho^2} + \frac{d_m}{r_m}\left(\frac{ik_T}{r_m}-\frac{1}{r^2}-\frac{1}{\rho^2}\right)e^{ik_T r_m}\right], \quad (53)$$

$$F_4(d_m) \approx \frac{4ik_1+2k_1^2 d_m}{(k_T^2-k_1^2)d_m}\left(\frac{e^{ik_1 d_m}}{\rho^2} - \frac{d_m}{r_m}\frac{e^{ik_1 r_m}}{\rho^2}\right) - \frac{4ik_1}{(k_T^2-k_1^2)d_m}\left(\frac{e^{ik_T d_m}}{\rho^2} - \frac{d_m}{r_m}\frac{e^{ik_T r_m}}{\rho^2}\right), \quad (54)$$

$$F_5(d_m) \approx -\frac{(2ik_1+k_1^2 d_m)\rho k_1}{(k_T^2-k_1^2)d_m}\left(\frac{1}{r_m^2}+\frac{i}{k_1 r_m^3}\right)e^{ik_1 r_m} + \frac{2ik_1 k_T\rho}{(k_T^2-k_1^2)d_m}\left(\frac{1}{r_m^2}+\frac{i}{k_T r_m^3}\right)e^{ik_T r_m}, \quad (55)$$

III. COMPUTATIONS AND DISSCUSIONS

Based on equations (36) to (41), the evaluations are carried out by invoking of I_1 to I_{10} in appendix and F_1 to F_5 by equation (51) to equation (55), respectively. To illustrate the approximated formulas, the formulas approximated are computed correspondingly in the following for electromagnetic components of ELF waves.

In Fig. 2, the electric components $E_{2\varphi}$ and $E_{2\rho}$ in dB are computed at specific distance ρ = 10 Km with the variant of observation heights z when the horizontal electric dipole source is located at the surface of anisotropic rock, as illustrated in Fig. 3. With the operating frequency at f = 3 Hz, the parameters of sea water are taken by the relative permittivity ε_{r1} = 80 and the conductivity σ_1 = 4 S/m, and the relative permittivity of anisotropic rock are assumed to be ε_{r2T} = ε_{r2L} = 10 and the conductivity (σ_x, σ_y, σ_z) of it are chosen by different directions. In Fig. 2, the blue solid and purple dot-dashed lines represent the one-dimensional anisotropic rock, in which the blue solid lines are for $\sigma_L < \sigma_T$ and the purple dot-dashed lines for the unavailable in physical but theoretical assumption $\sigma_L > \sigma_T$. The red dashed and green solid lines represent isotropic rock, respectively, and the red dashed lines are for the rock with lower conductivity and the green solid lines for the rock with high conductivity.

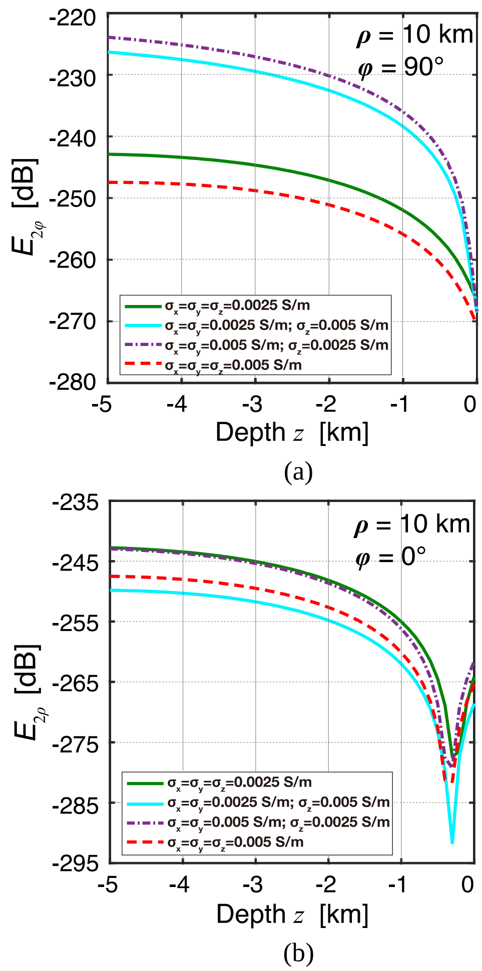

Fig. 2. Electric components of ELF field at specific distance in near zone due to a horizontal electric dipole versus the observation height on the surface of medium f = 3 Hz, ε_{r1} = 80, σ_1 = 4 S/m (Region 1 is sea), ε_{r2T} = ε_{r2L} = 10 (Region 2 is rock); d = 0 m, ρ = 10 Km, and φ = 0, $\pi/2$, respectively.

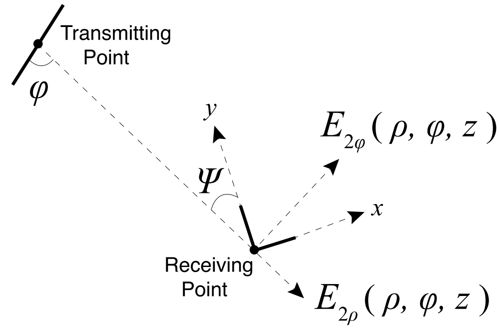

Fig. 3. The geometry and Cartesian coordinate system for a unit horizontal electric dipole excitation.

In Fig. 4, the computational results are compared with same parameters to the available experimental data addressed in [26]. The interesting experiment for detecting the subbed conductivity by the measurements of the ELF electric field on the ocean floor radiated by a horizontal antenna also on the ocean floor has been reported where the radial distance between the transmitting and receiving antennas is ρ = 18.9 Km, and the operating frequency is in the range of 0.25–2.5 Hz. The actually measured components E_X and E_Y can be expressed in the terms of the components $E_{1\rho}$ (ρ, φ, z) and $E_{1\varphi}$ (ρ, φ, z) of the field excited by the transmitter. We write:

$$E_X = E_{1\rho}(\rho,\varphi,z)\sin\psi + E_{1\varphi}(\rho,\varphi,z)\cos\psi, \quad (56)$$

$$E_Y = -E_{1\rho}(\rho,\varphi,z)\cos\psi + E_{1\varphi}(\rho,\varphi,z)\sin\psi. \quad (57)$$

In computations, we take ψ = 0° and φ = 0°, respectively.

In Fig. 4, the components E_X and E_Y vary as functions of the operating frequency. It is seen that for both the vectors E_X and E_Y only the blue solid lines are well in agreement with the measured data. For E_X, the blue solid and dot-dashed lines are nearly close together and both of them agree well with the measured data.

It is seen that E_X is not sensitive to the interchange of the two anisotropic models with $\sigma_L < \sigma_T$ and $\sigma_L > \sigma_T$. This is resulted by E_X being approximately equal to $E_{2\varphi}$ in the case of $\psi \sim 0$, and meanwhile the magnitudes of the terms including $e^{ik_L\rho}$ are approximately equal to those of the terms including $e^{ik_T\rho}$ at small radial distance (ρ = 10 km).

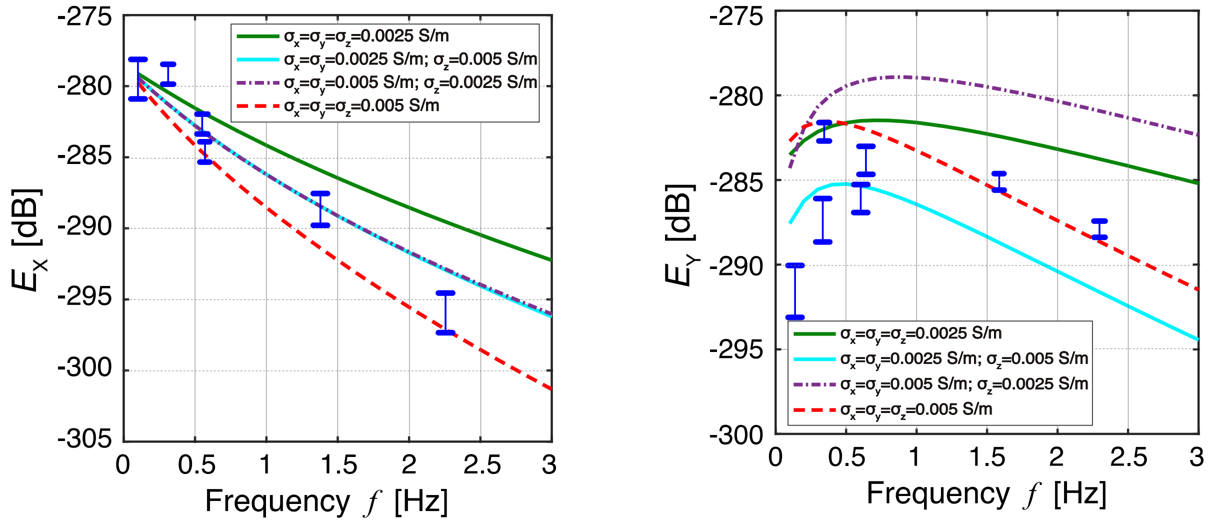

(a) (b)

Fig. 4. The comparison of the computational results by the proposed approximated formulas and ocean floor measurements by Young and Cox in 1981 [26].

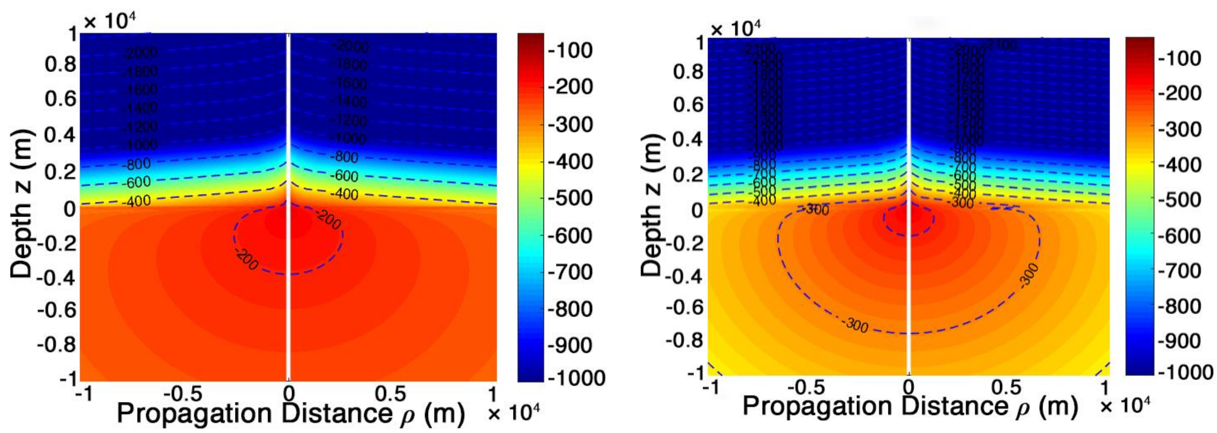

(a) with d = 0 m, σ_T = 0.0025 S/m, σ_L= 0.025 S/m (b) with d = 0 m, σ_T = 0.025 S/m, σ_L= 0.0025 S/m

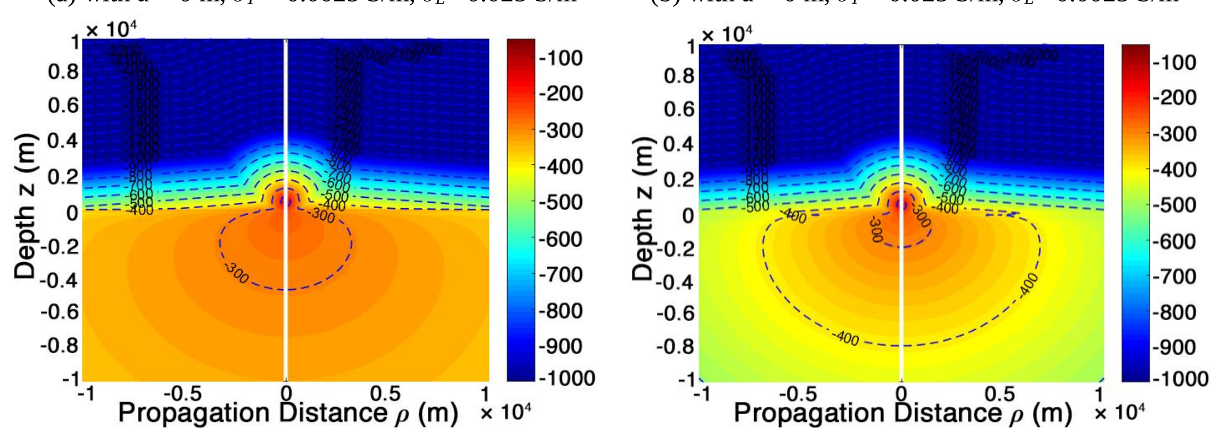

(c) with d = 500 m, σ_T= 0.0025 S/m, σ_L= 0.025 S/m (d) with d = 500 m, σ_T = 0.025 S/m, σ_L= 0.0025 S/m

Fig. 5. Projection of electric field component $|E_{2\rho}(\rho, \varphi, z)|$ with spatial distributions in $\hat{x}$ - $\hat{z}$ plane due to a horizontal electric dipole excitation in the presence of half-space regions, at f = 3 Hz, ε_{r1} = 80, σ_1 = 4 S/m (Region 1 is sea), ε_{r2T} = ε_{r2L} = 10 (Region 2 is rock); ρ = 10 Km, and φ = 0, d = 0 m, 500m, respectively.

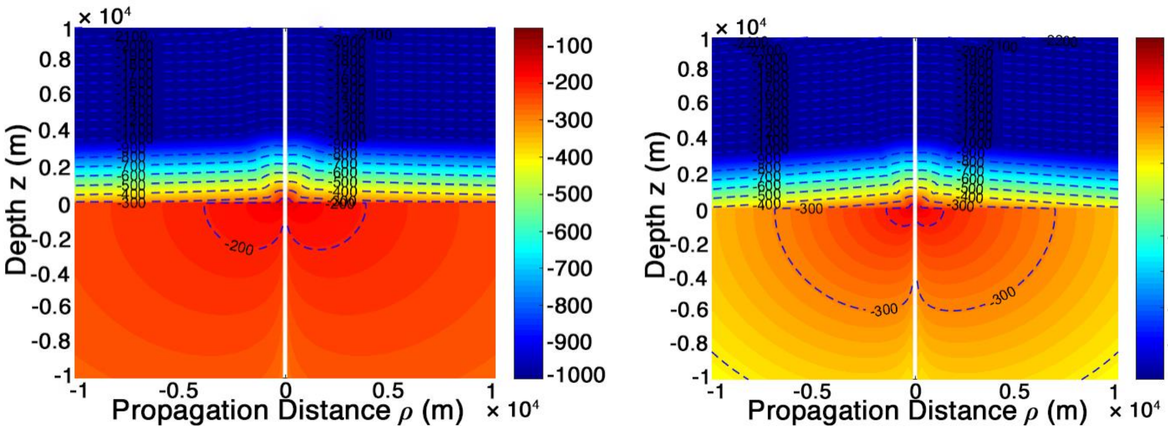

(a) with d = 0 m, σ_T = 0.0025 S/m, σ_L= 0.025 S/m

(b) with d = 0 m, σ_T = 0.025 S/m, σ_L= 0.0025 S/m

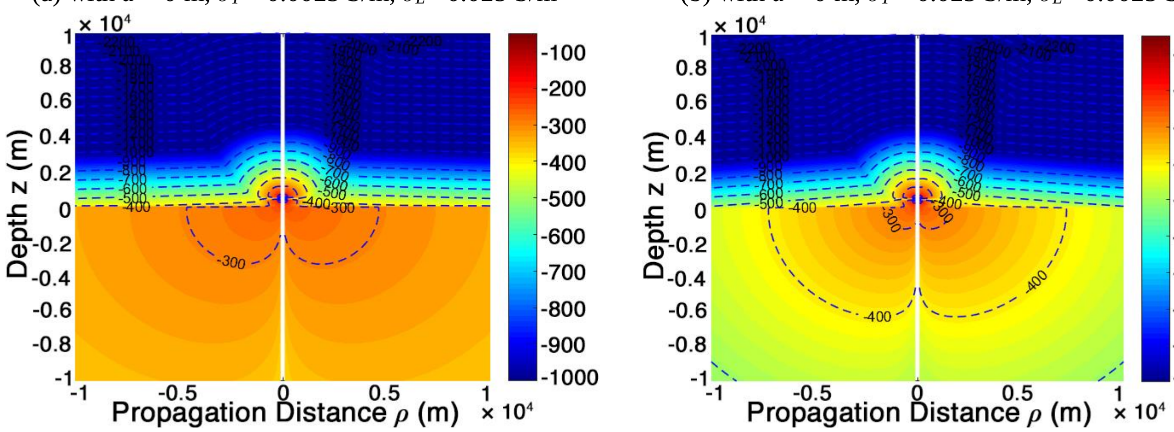

(c) with d = 500 m, σ_T = 0.0025 S/m, σ_L= 0.025 S/m

(d) with d = 500 m, σ_T = 0.025 S/m, σ_L= 0.0025 S/m

Fig. 6. Projection of electric field component $|E_{2z}(\rho, \varphi, z)|$ with spatial distributions due to a horizontal electric dipole excitation in the presence of half-space regions, at f = 3 Hz, ε_{r1} = 80, σ_1 = 4 S/m (Region 1 is sea), $\varepsilon_{r2T} = \varepsilon_{r2L}$ = 10 (Region 2 is rock); ρ = 10 Km, φ = 0, and d = 0 m, 500m, respectively.

Following the above computations and analyses, it may be reasonably concluded that the measured data are well represented as the one-dimensional anisotropic model and the reasonable values are with $\sigma_L \sim$ 0.002 to 0.0025 S/m and $\sigma_T \sim$ 0.004 to 0.005 S/m.

For illustration, the observation point is chosen arbitrarily on the $\hat{x}-\hat{z}$ plane, the distributions of the six components' strength for ELF wave due to horizontal electric dipole excitation in the presence of two half-spaces are depicted in Fig. 5 and Fig. 6, where a horizontal antenna of electric dipole is buried inside in the sea water at the height of d = 0 m and d = 500 m, respectively. With the operating frequency f = 3 Hz, the conductivity and the relative dielectric constant of sea water being σ_1 = 4 S/m, ε_{r1} = 80, respectively, and the relative dielectric constant of rock being approximately $\varepsilon_{r2T} = \varepsilon_{r2L}$ = 10 and the conductivity of it (σ_x, σ_y, σ_z) are chosen by different directions, the electromagnetic components vary as a function of propagating distance ρ and the height z of source. It is seen that the electromagnetic field decays dramatically due to high loss in sea water in Region 1, while it penetrates the rock floor in Region 2.

IV. CONCLUSIONS

In summary, the approximated formulas for ELF electromagnetic field have been derived in order to evaluate the ELF near field. The computational scheme exploits the concept that ELF near-field propagation can be simplified by the quasi-static approximation with $\gamma_2 \approx i\lambda$. Accordingly, the integrands of Fourier-Bessel representations for ELF field on the surface of the anisotropic rock are approximated by adopting Maclaurin's Expansion near the poles. The approximated solution is in good agreement with the available experimental data.

APPENDIX

The integrals of I_1 to I_{10} are addressed in [22], they are rewritten as follows:

$$I_1(k_n,d_m)=\int_0^\infty \frac{e^{ir_n d_m}}{r_n}J_0(\lambda\rho)\lambda d\lambda=-\frac{ie^{ik_n r_m}}{r_m}, \quad \text{(I1)}$$

$$\begin{aligned}I_2(k_n,d_m)&=\int_0^\infty \frac{e^{ir_n d_m}}{r_n}\left[J_0(\lambda\rho)-J_2(\lambda\rho)\right]\lambda^3 d\lambda\\&=-2k_n\left[\frac{ik_n}{r_m}-\frac{2}{r_m^2}-\frac{2i}{k_n r_m^3}\right.\\&\left.-\frac{d_m^2}{r_m^2}(\frac{ik_n}{r_m}-\frac{2}{r_m^2}-\frac{2i}{k_n r_m^3})\right]e^{ik_n r_m}\end{aligned}, \quad \text{(I2)}$$

$$\begin{aligned}I_3(k_n,d_m)&=\int_0^\infty \frac{e^{ir_n d_m}}{r_n}\left[J_0(\lambda\rho)+J_2(\lambda\rho)\right]\lambda^3 d\lambda\\&=-2k_n(\frac{1}{r_m^2}+\frac{i}{k_n r_m^3})e^{ik_n r_m}\end{aligned}, \quad \text{(I3)}$$

$$\begin{aligned}I_4(k_n,d_m)&=\int_0^\infty e^{ir_n d_m}J_1(\lambda\rho)\lambda^2 d\lambda\\&=-\rho k_n\frac{d_m}{r_m}(\frac{k_n}{r_m^2}+\frac{3i}{r_m^3}-\frac{3}{k_n r_m^4})e^{ik_n r_m}\end{aligned}, \quad \text{(I4)}$$

$$\begin{aligned}I_5(k_n,d_m)&=\int_0^\infty e^{ir_n d_m}J_0(\lambda\rho)\lambda d\lambda\\&=-\frac{d_m}{r_m}(\frac{ik_n}{r_m}-\frac{1}{r_m^2})e^{ik_n r_m}\end{aligned}, \quad \text{(I5)}$$

$$\begin{aligned}I_6(k_n,d_m)&=\int_0^\infty e^{ir_n d_m}\left[J_0(\lambda\rho)+J_2(\lambda\rho)\right]\lambda d\lambda\\&=2(\frac{e^{ik_n d_m}}{\rho^2}-\frac{d_m}{r_m}\frac{e^{ik_n r_m}}{\rho^2})\end{aligned}, \quad \text{(I6)}$$

$$\begin{aligned}I_7(k_n,d_m)&=\int_0^\infty e^{ir_n d_m}\left[J_0(\lambda\rho)+J_2(\lambda\rho)\right]\lambda d\lambda\\&=-2\left[\frac{e^{ik_n d_m}}{\rho^2}+\frac{d_m}{r_m}\left(\frac{ik_n}{r_m}-\frac{1}{r_m^2}-\frac{1}{\rho^2}\right)e^{ik_n r_m}\right]\end{aligned}, \quad \text{(I7)}$$

$$\begin{aligned}I_8(k_n,d_m)&=\int_0^\infty \frac{e^{ir_n d_m}}{r_n}J_1(\lambda\rho)\lambda^2 d\lambda\\&=-\rho k_n\left(\frac{1}{r_m^2}+\frac{i}{k_n r_m^3}\right)e^{ik_n r_m}\end{aligned}, \quad \text{(I8)}$$

$$\begin{aligned}I_9(k_n,d_m)&=\int_0^\infty r_n e^{ir_n d_m}\left[J_0(\lambda\rho)-J_2(\lambda\rho)\right]\lambda d\lambda\\&=-2k_n\left\{\frac{e^{ik_n d_m}}{\rho^2}+\left[\frac{1}{r_m^2}+\frac{i}{k_n r_m^3}\right.\right.\\&\left.\left.+\frac{d_m^2}{r_m^2}\left(\frac{ik_n}{r_m}-\frac{3}{r_m^2}-\frac{3i}{k_n r_m^3}-\frac{1}{\rho^2}\right)\right]e^{ik_n r_m}\right\}\end{aligned}, \quad \text{(I9)}$$

$$\begin{aligned}I_{10}(k_n,d_m)&=\int_0^\infty r_n e^{ir_n d_m}\left[J_0(\lambda\rho)+J_2(\lambda\rho)\right]\lambda d\lambda\\&=2k_n\left[\frac{e^{ik_n d_m}}{\rho^2}+\frac{ie^{ik_n r_m}}{k_n r_m^3}\left(1+\frac{ik_n r_m d_m^2}{\rho^2}\right)\right]\end{aligned}, \quad \text{(I10)}$$

where m = 0, 1 and n = 0, 1.

ACKNOWLEDGMENT

This work was supported by the [National Natural Science Foundation of China] under Grant [number 61271086, 61571389].

REFERENCES

[1] A. N. Sommerfeld, "Propagation of waves in wireless telegraphy," *Ann. Phys.*, vol. 28, pp. 665-736, Mar. 1909.

[2] S. F. Mahmoud, "Remarks on 'The electromagnetic field of a vertical electric dipole over the earth and sea'," *IEEE Trans. Antennas Propagat.*, vol. 46, no. 12, pp. 1745-1946, Apr. 1999.

[3] W. Y. Pan, "Surface wave propagation along the boundary between sea water and one dimensionally anisotropic rock," *J. Appl. Phys.*, vol. 58, pp. 3963-3974, 1985.

[4] T. T. Wu and R. W. P. King, "Lateral electromagnetic pulses generated by a vertical dipole on the boundary between two dielectrics," *J. Appl. Phys.*, vol. 62, no. 11, pp. 4345-4355, June 1998.

[5] R. W. P. King, M. Owens, and T. T. Wu, *Lateral Electromagnetic Waves: Theory and Applications to Communications, Geophysical Exploration, and Remote Sensing*. Springer, New York, 1992.

[6] D. Margetis and T. T. Wu, "Exactly calculable field components of electric dipoles in planar boundary," *Journal of Mathematical Physics*, vol. 42, no. 2, pp. 713-745, Jan. 2001.

[7] D. Margetis, "Radiation of horizontal electric dipole on large dielectric sphere," *Journal of Mathematical Physics*, vol. 43, no. 6, pp. 3162-3201, May 2002.

[8] H. Q. Zhang, W. Y. Pan, K. Li, and K. X. Shen, "Electromagnetic field for a horizontal electric dipole buried inside a dielectric layer coated high lossy half space," *Progress in Electromagnetics Research*, *PIER*, vol. 50, pp. 163-186, 2005.

[9] K. Li and Y. Lu, "Electromagnetic field generated by a horizontal electric dipole near the surface of a planar perfect conductor coated with a layer," *IEEE Trans. Antennas Propagt.*, vol. 53, no. 10, pp. 3191-3200, 2005.

[10] J. P. Mei and K. Li, "Electromagnetic field from a horizontal electric dipole on the surface of a high lossy dielectric coated with a layer," *Progress in Electromagnetics Research*, *PIER*, vol. 73, pp. 71-91, 2007.

[11] J. L. Tang and W. Hong, "The electromagnetic field produced by a horizontal electric dipole over a dielectric coated perfect conductor," *Progress in Electromagnetics Research*, *PIER*, vol. 36, pp. 139-152, 2002.

[12] M. Fechner, N. A. Spaldin, and I. E. Dzyaloshinskii, "Magnetic field generated by a charge in a magnetoelectric material," *Phys. Rev. B*, vol. 89, no. 18, pp. 1719-1743, 2014.

[13] Y. L. Geng, C. W. Qiu, and N. Yuan, "Exact

solution to electromagnetic scattering by an impedance sphere coated with a anisotropic layer," *IEEE Trans. on Antennas Propagat.*, vol. 57, no. 2, pp. 572-576, 2009.
[14] M. Parise, "Second-Order formulation for the quasi-static field from a vertical electric dipole on a lossy half-space," *Progress in Electromagnetics Research*, vol. 140, no. 4, pp. 439-455, June 2013.
[15] M. Parise, "An exact series representation for the EM field from a vertical electric dipole on an imperfectly conducting half-space," *Journal of Electromagnetic Waves and Applications*, vol. 28, no. 8, pp. 932-942, Mar. 2014.
[16] J. J. Simpson and A. Taflove, "ELF radar system proposed for localized D-region ionospheric anomalies," *IEEE Geoscience and Remote Sensing Letters*, vol. 3, no. 4, pp. 500-503, Oct. 2006.
[17] J. J. Simpson, "Current and future applications of 3-D global earth-ionosphere models based on the full-vector Maxwell's equations FDTD method," *Surv. Geophys*, vol. 30, no. 2, pp. 105-130, Mar. 2009.
[18] J. J. Simpson and A. Taflove, "A novel ELF radar for major oil deposits," *IEEE Geoscience and Remote Sensing Letters*, vol. 3, no. 1, pp. 36-39, Jan. 2006.
[19] Y. Wang, H. Xia, and Q. Cao, "Analysis of ELF propagation along the earth surface using the FDTD model based on the spherical triangle meshing," *IEEE Antennas Wireless Propagat. Lett.*, vol. 8, no. 4, pp. 1017-1020, Sept. 2009.
[20] Y. Wang, H. Xia, and Q. Cao, "Analysis of ELF attenuation rate using the geodesic FDTD algorithm," *International Conference on Microwave and Millimeter Wave Technology*, *IEEE*, pp. 1413-1415, July 2010.
[21] Y. Wang, Q. Cao, and B. Su, "A quasi three-dimensional subgrid technique for the geodesic FDTD algorithm," *International Symposium on Antennas, Propagation & EM Theory*, *IEEE*, pp. 936-938, Jan. 2013.
[22] W. Y. Pan and K. Li, "ELF wave propagation along sea-rock boundary and mCSEM method," in *Propagation of SLF/ELF Electromagnetic Waves*, 1st ed. Hangzhou, CN: Zhejiang University Press; Berlin Heidelberg, GER: Springer-Verlag, ch. 6, pp. 161-219, 2014.
[23] E. I. Parkhomenko, *Electrical Properties of Rocks*. Plenum, New York, 1967.
[24] H. L. Xu, T. T. Gu, and K. Li, "Approximated solutions for ELF near-field propagation due to a horizontal electric dipole excitation near the sea-rock boundary," *IEEE Trans. on Antennas Propagat.*, vol. 66, no. 5, pp. 2471-2481, May 2018.
[25] J. R. Wait, *Electromagnetic Waves in Stratified Media*. 2nd ed., New York: Pergamon Press, 1970.
[26] P. D. Young and C. S. Cox, "Electromagnetic active source sounding near the East Pacific Rise," *Geophys. Res. Lett.*, vol. 8, no. 10, pp. 1043-1046, Oct. 1981.

Ting Ting Gu was born in Leshan, Sichuan, China, on June 18, 1988. She received the B.S. degree and M.S. degree in Electromagnetic Field and Microwave Technology from Zhejiang University of Media and Communications, and Hangzhou Dianzi University, Hangzhou, China, in 2010 and 2013, respectively.

She is currently working toward the Ph.D. degree in Electromagnetic Field and Microwave Technology with the College of Information Science and Electronic Engineering, Zhejiang University, Hangzhou, China. Her current research interests include radio wave propagation theory and its applications.

Hong Lei Xu was born in Jiangyin, Jiangsu, China, on June 7, 1990. She received the B.S. degree in Communication Engineering from Nanjing University of Posts and Telecommunications, Nanjing, China, in 2012, and the M.S. degree in Jiangsu University, Zhenjiang, China, in 2015, respectively.

She is currently working toward the Ph.D. degree in Electromagnetic Field and Microwave Technology with the College of Information Science and Electronic Engineering, Zhejiang University, Hangzhou, China. Her current research interests include radio wave propagation theory and its applications.

Kai Li was born in Xiao County, Anhui, China, on February 10, 1968. He received the B.S. degree in Physics from Fuyang Normal University, Anhui, China, in 1990, the M.S. degree in Radio Physics from Xidian University, Xi'an, Shaanxi, China, in 1994, and the Ph.D. degree in Astrophysics from Shaanxi Astronomical Observatory, the Chinese Academy of Sciences, Shaanxi, China, in 1998, respectively.

From August 1990 to December 2000, he was on the Faculty of China Research Institute Radiowave Propagation (CRIRP). From January 2001 to December 2002, he was a Postdoctoral Fellow at Information and

Communications University (ICU), Daejeon, Republic of Korea. From January 2003 to January 2005, he was a Research Fellow with the School of Electrical and Electric Engineering, Nanyang Technological University (NTU), Singapore. Since January 2005, he has been a Professor with the Department of Information Science and Electronic Engineering, Zhejiang University, Hangzhou, China. His current research interests include classic electromagnetic theory and radio wave propagation.

Li is a Senior Member of the Chinese Institute of Electronics (CIE) and a Member of the Chinese Institute of Space Science (CISS).